

Simulation of optical and X-ray sum frequency generation spectroscopy of one-dimensional molecular chain

Satoshi Tanaka^{a,*}, Shaul Mukamel^b

^a Department of Materials Science, College of Integrated Arts and Science, Osaka Prefecture University, Sakai 599-8531, Osaka, Japan

^b Department of Chemistry, University of California Irvine, Irvine, CA 92697-2025, USA

Abstract

The time-resolved sum frequency generation signal of an optical and X-ray pulse is calculated for a one-dimensional molecular chain. We show how the valence exciton motion induced by the first optical light pulse can be probed with atomic scale precision by tuning the X-ray frequency across a core excitation of a particular atom. This technique provides a novel real-time, real-space probe for dynamics of valence excitation in a single molecule.

© 2004 Elsevier B.V. All rights reserved.

Keywords: Time-resolved sum frequency generation; X-ray pulse; Valence exciton motion

1. Introduction

Recent rapid progress in the development of coherent ultrafast X-ray pulses have opened up a new era in X-ray spectroscopy [1,2]. As pulse intensities and coherence properties are improved, ultrafast resonant spectroscopy with X-ray pulses has become feasible. Combination of femtosecond optical light pulse and attosecond X-ray pulse makes it possible to investigate electron motions in atoms, molecules, and solid state materials in real space and real time. The high temporal (attosecond) and spatial (sub-nanometer) resolution of these techniques offers a new window into molecular structure and dynamical processes. Structural changes induced by optical excitation have been investigated by time-resolved X-ray diffraction and time-resolved X-ray absorption spectroscopies [3–6].

We propose and simulate new non-linear X-ray spectroscopy whereby ultrafast electronic relaxation process induced by optical excitation can be investigated using real-time snapshots with atomic scale precision by time-resolved sum frequency generation (SFG), which combines optical and X-ray pulses. We demonstrate its utility as

a novel probe for electronic motions in a one-dimensional molecular chain model.

In the proposed technique, the second-order non-linear polarization induced by two radiation fields, an optical light pulse with a wave vector \mathbf{k}_1 and a X-ray pulse with a wave vector \mathbf{k}_2 , is detected with variable time delay between these pulses (Fig. 1). By tuning the X-ray frequency to the core excitation of a particular atom, a valence exciton wave packet motion can be launched and probed at the targeted atomic site.

2. Expressions of SFG signal

Expression for the SFG signal is derived from the general formulation of a non-linear X-ray spectroscopy in terms of the non-linear response functions [7]. We consider heterodyne detection where the resulting non-linear polarization is mixed with a local oscillator in order to gain sensitivity [8]. The incoming electric field is

$$E(\mathbf{r}, t) = E_1(t + \tau) \exp[i(\mathbf{k}_1 \cdot \mathbf{r} - \omega_1 t)] + E_2(t) \exp[i(\mathbf{k}_2 \cdot \mathbf{r} - \omega_2 t)] + E_{LO}(t - \tau') \times \exp[i(\mathbf{k}_{LO} \cdot \mathbf{r} - \omega_{LO} t)] + \text{c.c.}, \quad (1)$$

where \mathbf{k} and ω denote the wave vector and central frequency of the incoming fields.

* Corresponding author. Tel.: +81-722-52-1161; fax: +81-722-54-9710.

E-mail address: stanaka@ms.cias.osakafu-u.ac.jp (S. Tanaka).

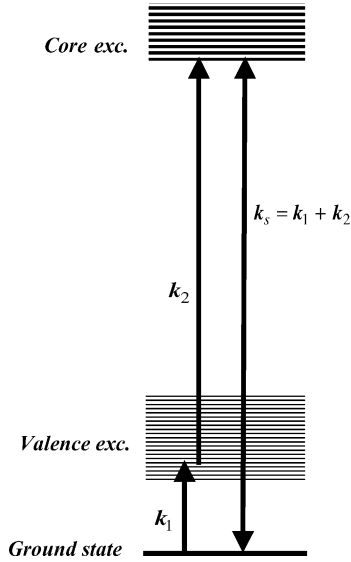


Fig. 1. Process scheme of sum frequency generation spectroscopy with a combination of optical pulse k_1 and X-ray pulse k_2 . The signal is measured by heterodyne detection in the direction of $k_s = k_1 + k_2$. Optical light and X-ray pulses are resonant with valence exciton and core exciton states, respectively.

The heterodyne SFG signal is given by

$$S_{\text{SFG}}(\mathbf{k}_s, \tau) = -2\omega_s \text{Im} \int_{-\infty}^{\infty} dt E_{\text{LO}}^*(t) P^{(2)}(\mathbf{k}_s, t) \times \exp[i(\omega_{\text{LO}} - \omega_s)t], \quad (2)$$

where $\mathbf{k}_s = \mathbf{k}_1 + \mathbf{k}_2$ and $\omega_s = \omega_1 + \omega_2$. The second-order polarization $P^{(2)}(\mathbf{k}_s, t)$ in Eq. (2) is expressed in terms of the non-linear response functions given in Appendix A in [7].

The second-order non-linear polarization is generated as a sum of the fields of a optical laser pulse which comes first and a subsequent X-ray pulse. The SFG signal intensity Eq. (2) under rotating wave approximation (RWA) can be expressed as

$$S_{\text{SFG}}(\mathbf{k}_s; \tau) = \frac{2}{\hbar^2} \frac{1}{\omega_2 \omega_1 \omega_s} \text{Re} \int_{-\infty}^{\infty} dt \int_0^{\infty} dt_2 \times \int_0^{\infty} dt_1 Q(-\mathbf{k}_s; \mathbf{k}_2, \mathbf{k}_1, t_2, t_1) \times \exp[i(\omega_2 + \omega_1)t_2 + i\omega_1 t_1] E_{\text{LO}}^*(t - \tau') \times E_2(t - t_2) E_1(t - t_2 - t_1 + \tau), \quad (3)$$

where the non-linear response function is

$$Q(-\mathbf{k}_s; \mathbf{k}_2, \mathbf{k}_1, t_2, t_1) = \langle \hat{j}(\mathbf{r}, t_2 + t_1) \hat{j}(\mathbf{r}_2, t_1) \hat{j}(\mathbf{r}_1, 0) \rangle. \quad (4)$$

Assuming that the two pulses are temporally well separated, the SFG signal intensity is given by *doorway–window representation* [8] as

$$S_{\text{SFG}}(\mathbf{k}_s; \tau) = \frac{-2}{\hbar} \text{Re} \sum_{g'} W_{eg'}(\omega_1, \omega_2) \times \exp[i\omega_1 \tau] I_{g'g}(\tau) D_{g'g}(\omega_1), \quad (5)$$

where g, g' and e denote the ground, optically-excited, and core excited states, respectively. Here, $D_{g'g}(\omega_1)$ is the doorway function representing the exciton wave packet created by the first pulse

$$D_{g'g}(\omega_1) \equiv \frac{i}{\hbar} \sum_{e=e_a, e_b} J_{ge;eg'}^*(\mathbf{k}_1 - \mathbf{k}_2) \times \int_{-\infty}^{\infty} dt' \int_0^{\infty} dt_1 \times \exp[i(\omega_2 - \omega_1)t' + i\omega_1 t_1] \times E_2^*(t') E_1(t' - t_1) I_{g'g}(-t') I_{eg}(t_1), \quad (6)$$

whereas $W_{eg'}(\omega_1, \omega_2)$ is the *window function* representing the generation of the signal

$$W_{eg'}(\omega_1, \omega_2) \equiv \frac{i}{\hbar} \sum_{e=e_a, e_b} J_{ge;eg'}(\mathbf{k}_1 - \mathbf{k}_2) \times \int_{-\infty}^{\infty} dt \int_0^{\infty} dt_3 \times \exp[-i(\omega_2 - \omega_1)t + i(\omega_3 - \omega_2 + \omega_1)t_3] \times E_{\text{LO}}^*(t + t_3) E_3(t) I_{eg}(t_3) I_{g'g}(t). \quad (7)$$

In Eqs. (6) and (7), $I_{ab}(t)$ is an auxiliary function representing the time evolution of the density matrix

$$I_{ab}(t) \equiv \theta(t) \exp[-i\omega_{ab}t - \Gamma_{ab}t], \quad (8)$$

with the transition frequency $\hbar\omega_{ab} = \epsilon_a - \epsilon_b$ and dephasing rate for the ab transition $\Gamma_{ab} = (1/2)(\gamma_a + \gamma_b) + \hat{\Gamma}_{ab}$ are introduced. γ_a and γ_b are the inverse lifetimes of the a and b states, and $\hat{\Gamma}_{ab}$ is the *pure dephasing* matrix. $J_{ab;cd}(\mathbf{k})$ is a tetradic current density matrix defined by [9]

$$J_{ab;cd}(\mathbf{k}) \equiv \int d\mathbf{r} j_{ab}(\mathbf{r}) j_{cd}^*(\mathbf{r}) \exp(-i\mathbf{k} \cdot \mathbf{r}), \quad (9)$$

with $j_{ab}(\mathbf{r}) \equiv \langle a | \hat{j} | b \rangle$ is a current density operator matrix.

3. The model

We have simulated the time-resolved SFG signal in a one-dimensional molecular chain with N atoms, each having a core orbital, an occupied valence orbital, and an unoccupied conduction orbital, as shown in Fig. 2. In the Hamiltonian we include the transfer of the conduction electron (t_c) and valence hole (t_v), but neglect core hole transfer. The on-site attractive Coulomb interactions between a core hole and a conduction electron (core exciton effect) (U_{ca}), between the valence hole and a conduction electron (valence exciton effect) (U_{cv}). By eliminating the indices for spin degeneracy which only cause additional multiplicity, the total Hamiltonian reads

$$\hat{H}_m = - \sum_{l=1}^N \epsilon_{a,l} a_l^\dagger a_l + \sum_{l=1}^N \epsilon_{v,l} v_l^\dagger v_l - \sum_{l=1}^N \epsilon_{c,l} c_l^\dagger c_l + t_v \sum_{l,m=1, l \neq m}^N v_l^\dagger v_m + t_c \sum_{l,m=1, l \neq m}^N c_l^\dagger c_m - \sum_{l=1}^N U_{ca} c_l^\dagger c_l (1 - a_l^\dagger a_l) - \sum_{l=1}^N U_{cv} c_l^\dagger c_l (1 - v_l^\dagger v_l). \quad (10)$$

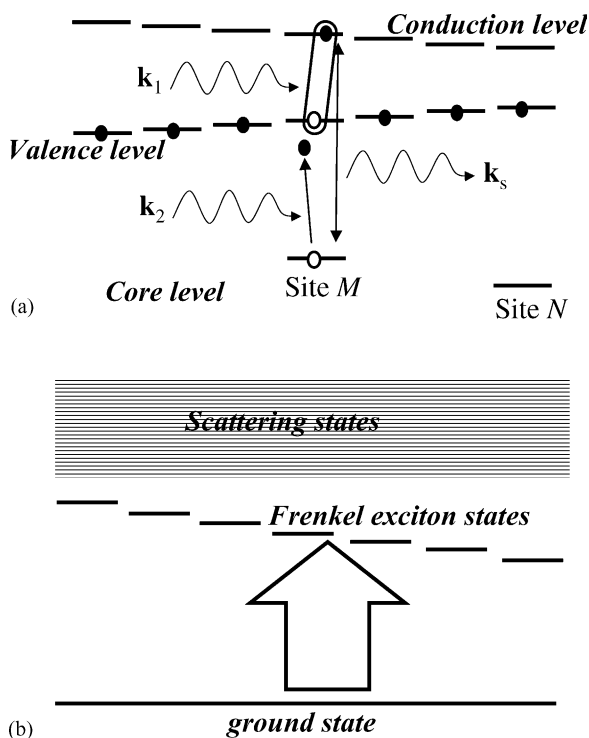


Fig. 2. Level structure of a one dimensional molecular chain model system (a). Optical pulse comes first to induce a valence exciton excitation and the motion is detected at a particular atomic site by resonant X-ray pulse. The Frenkel exciton states lie lower in energy than scattering states (b).

As a model system, we consider a molecular chain with $N = 30$ and the following parameters: $t_c = -2.0$, $t_v = 1.5$, $U_{ca} = 3.0$, and $U_{cv} = 7.0$ (in eV). These values yield the Frenkel exciton states below the scattering states shown in Fig. 2(b).

One of the keys to manufacturing molecular electronic devices is how to design the molecular electronic structure to effectively transfer an absorbed energy from light within a molecule [10,11]. In energy-funnel molecules, as dendrimeric nanostars [12,13], the highly effective energy transfer from the peripheral end to a reaction center is realized through the gradual change of Frenkel exciton site energy. In order to mimic such an Frenkel exciton energy landscape in a molecule, we assume that the site energies for the conduction ($\epsilon_{c,l}$) and valence ($\epsilon_{v,l}$) levels increase and decrease linearly with the atomic position, respectively, resulting in the red shifted Frenkel exciton site energies from left to right as shown in Fig. 2(b).

The eigenstates of \hat{H}_m were computed by direct diagonalization using the basis set for the single core excited states and the valence exciton states introduced in [9]. To allow spectral selectivity, we assumed that the core excited state energies of site M ($\epsilon_M = -100$ eV), which is a middle of the molecule, and site N ($\epsilon_N = -150$ eV), which is the right end of the molecule, are well separated (Fig. 2(a)). The SFG signal was calculated by Eq. (5) using the sum-over-state expression.

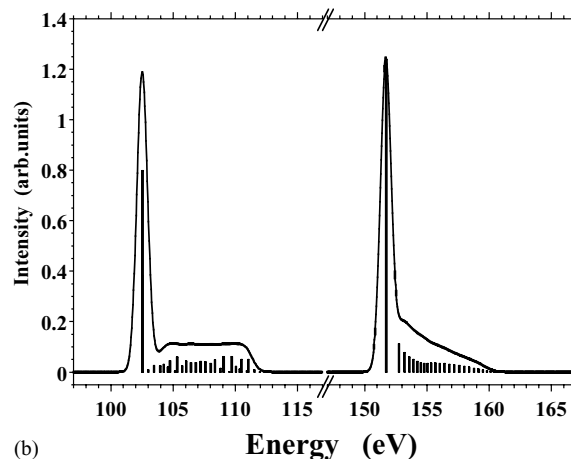
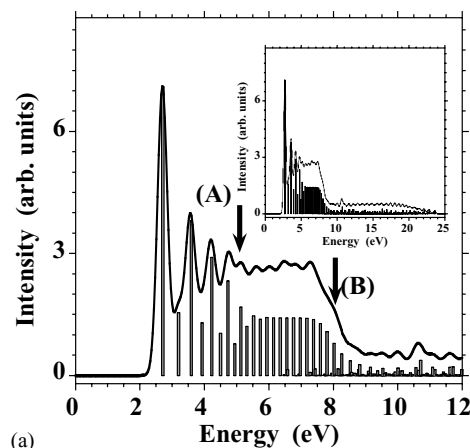


Fig. 3. The calculated optical absorption spectrum (a), and X-ray absorption spectra (b). The overall profile of the optical absorption spectrum is shown in the inset in (a). The arrows A and B indicate the central frequencies of optical light pulses.

4. Numerical results

The calculated low energy range of optical absorption is shown in Fig. 3(a), and the overall absorption spectrum is shown in the inset. The absorption spectrum shows Frenkel exciton states below 8.5 eV and scattering states at higher energies.

In Fig. 3(b), we show the calculated X-ray absorption for the core excitations at sites M and N . Since the core levels are energetically well separated from each other, we can selectively excite the molecule at each atomic site by tuning the X-ray frequencies across the core frequencies. The intense lowest energy peaks for both X-ray absorption spectra correspond to the transition to the strongly localized core exciton states.

In order to illustrate the time evolution of the valence exciton motion induced by optical light pulse, we have further calculated the time evolution of the reduced density matrix

$$\rho_{nl}(\tau) = \text{Tr}[c_n v_l^\dagger \hat{\rho}(\omega_1; \tau)], \quad (11)$$

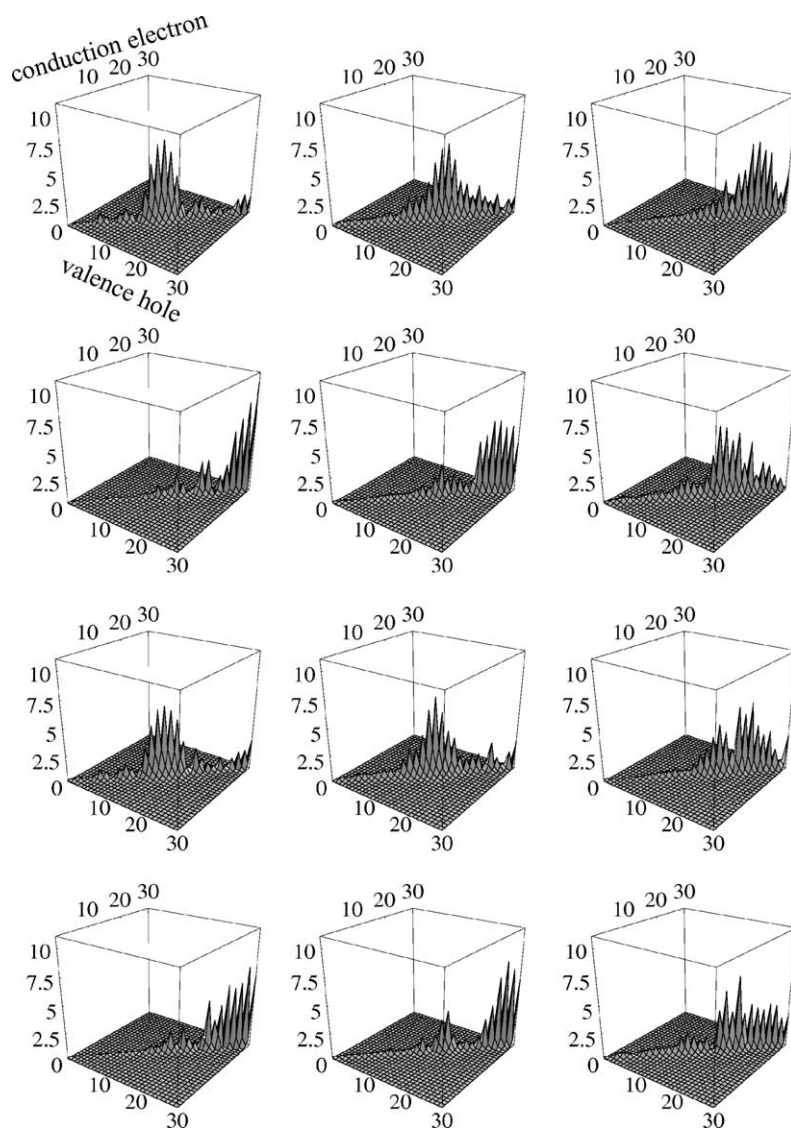


Fig. 4. Time evolution of $|\rho_{nl}(\tau)|$ for $\omega_1 = 5.12$ eV with varying τ from 0 to 40 fs, from left top to right bottom. Time step is 3.3 fs. Plane axes stand for the site numbers of valence hole and conduction electron.

where $\rho_I(\omega_1; \tau)$ is the exciton density operator defined by

$$\hat{\rho}(\omega_1; \tau) = \exp[i\omega_1 \tau] \sum_{g'} I_{g'g}(\tau) D_{g'g}(\omega_1) |g' \rangle \langle g|. \quad (12)$$

The diagonal matrix elements represent the net charge and the off-diagonal elements represent the bond-order induced by the optical transition [14].

In Fig. 4, we show the time evolution of $|\rho_{nl}(\tau)|$ for $\omega_1 = 5.12$ eV marked with the arrow A in Fig. 3(a). The envelope function for the optical pulse, $E_1(t)$, is assumed to be rectangular with 5 fs duration. The axes in the plane denote the site numbers for a valence hole and conduction electron. Time proceeds from left to right and from top to bottom with a 3.3 fs time step.

Since the valence exciton wave packet is initially created by tuning ω_1 to the middle of the Frenkel exciton band, the valence exciton propagates through Frenkel exciton bands,

as is clearly shown in the figure: diagonal matrix elements dominate the off-diagonal matrix elements in Fig. 4. The valence exciton wave packet is created around the center of the molecule by the optical light pulse, and it moves towards site N , and back to the original position. Since there is no dissipation in the model, the coherent wave packet motion persists with about 20 fs period of time.

The time-resolved SFG signal clearly reflects this coherent valence exciton motion. The calculated SFG for $\omega_1 = 5.12$ eV is shown in Fig. 5 where central frequencies of X-ray pulse ω_2 are tuned such that the signal frequency $\omega_s = \omega_1 + \omega_2$ is tuned with the core exciton peak at site M (solid line) and site N (dotted line), i.e. $\omega_2 = 97.4$ eV (site M , solid line) and $\omega_2 = 146.6$ eV (site N , dotted line). The X-ray and optical pulse envelopes were assumed to be the same.

We clearly see that at $\tau = 0$ the amplitude of the solid line is larger than the dotted line. This is consistent with

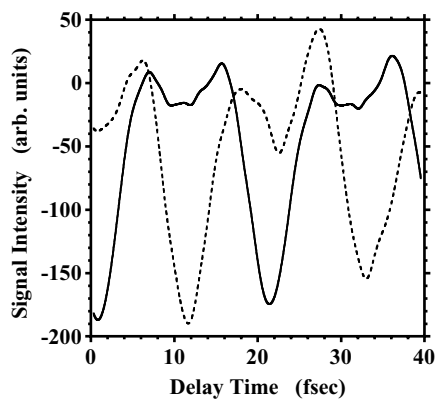


Fig. 5. Time-resolved SFG signal for $\omega_1 = 5.12$ eV. Solid and dotted lines are obtained when X-ray pulse frequencies are resonant with core excitation frequencies of site M and N , respectively.

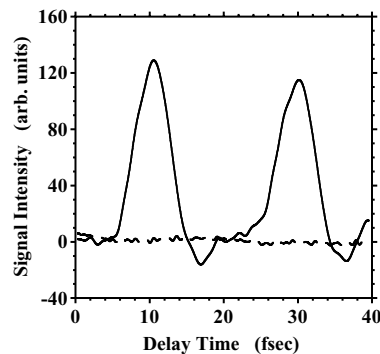


Fig. 7. Time-resolved SFG signal for $\omega_1 = 8.02$ eV. Solid and dotted lines are obtained when X-ray pulse frequencies are resonant with core excitation frequencies of site M and N , respectively.

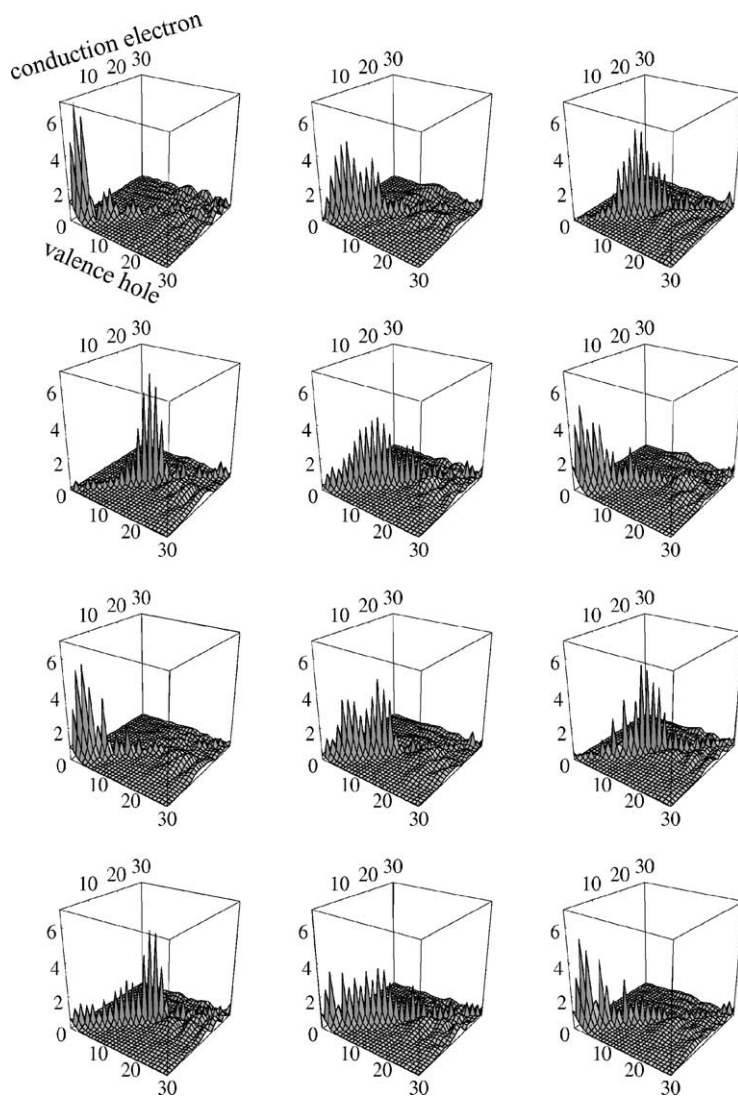


Fig. 6. Time evolution of $|\rho_{nl}(\tau)|$ for $\omega_1 = 8.02$ eV with varying τ from 0 to 40 fs, from left top to right bottom. Time step is 3.3 fs. Plane axes stand for the site numbers of valence hole and conduction electron.

the feature of the left top panel of Fig. 4: the wave packet amplitude is large at the site M and small at site N . At longer delay times, the SFG signal probed at site M decreases while at site N it increases, corresponding to the wave packet transports from the center to the right end as shown in Fig. 4. The amplitude at site M recovers again, while that at site N is reduced. These temporal changes repeat with 20 fs period. SFG thus probes the valence exciton motion after optical excitation with atomic scale precision.

In Fig. 6, we show the time evolution of $|\rho_{nl}(\tau)|$ when $\omega_1 = 8.02$ eV. Since ω_1 is tuned with the higher energy of the Frenkel exciton state, the amplitude concentrates at the left end site at $\tau \simeq 0$. As time evolves the center of the wave packet shifts to the right, but the main part of the wave packet returns back before it reaches to the right end (site N). Since ω_1 is tuned to the border between Frenkel exciton states and scattering states, the value of off-diagonal elements of $\rho(\tau)$ are also visible. The SFG calculated for this ω_1 shown in Fig. 7 is consistent with this wave packet motion: the SFG signal probed at site M (solid line) oscillates with large amplitude, while the intensity probed at site N (dotted line) is very weak. The clear difference between Figs. 5 and 7 illustrates that this technique directly probes the dependence of the valence exciton motion on the excitation energy.

5. Summary

In the present work we have presented a novel technique for probing a valence exciton motion in one-dimensional molecular chain induced by optical pulse excitation with atomic scale precision; the second-order non-linear polarization is measured by a frequency sum of optical and X-ray pulses. By tuning the X-ray frequency across a core excitation energy of a particular atom, we can detect the valence exciton wave packet at that targeted atomic site as a function of the delay time of X-ray pulse with regards to the pump-optical pulse.

It should be noted that this is a purely coherent spectroscopy which probes a coherent valence exciton motion in a molecule. This coherent valence exciton motion may be damped by the coupling to thermal bath mode. The dephasing time has been probed by many ultrafast optical techniques and was found to be about several picoseconds in many mesoscopic systems [15]. The SFG signal computed here assumed this dephasing time. This is made possible with use of femtosecond optical and X-ray pulses, as shown in Figs. 5 and 7.

It will be very interesting to investigate the two types of the transport mechanism in a molecule: incoherent hopping and coherent transport [16–18]. Ultrafast optical spectroscopy, such as time-resolved fluorescence, is indeed a useful probe to distinguish between these two mechanisms [16], but it cannot directly probe the spatial coherence between different atomic sites within a molecule because of the long wavelength limit. The present technique may reveal temporal and spatial coherence of the optically excited state in a molecule, and provides us with most valuable information on molecular charge transport.

Acknowledgements

We thank Prof. Y. Kayanuma for valuable discussions. This work is partially supported by the Grant-in-Aid from the Ministry of Education, Culture, Sports, Science, and Technology in Japan. The support of the US Department of Energy, Chemical Science Division DE-FG02-01ER 15155 is gratefully acknowledged.

References

- [1] T. Brabec, F. Krausz, *Rev. Mod. Phys.* 72 (2000) 545.
- [2] M. Drescher, M. Hentschel, R. Kienberger, G. Tempea, C. Spielmann, A.G. Reider, P.B. Corkum, F. Krausz, *Science* 291 (2001) 1923.
- [3] P.M. Rentzepis, J. Helliwell, *Time-Resolved Electron and X-ray Diffraction*, Oxford Press, New York, 1995.
- [4] A. Rousse, C. Rischel, J.-G. Gauthier, *Rev. Mod. Phys.* 73 (2001) 17.
- [5] L.X. Chen, W.J.H. Jäger, G. Jennings, D. J Gosztola, A. Munkholm, J.P. Hessler, *Science* 292 (2001) 262.
- [6] M. Saes, C. Bressler, R. Abela, D. Grolimund, S.L. Johnson, P.A. Heimann, M. Chergui, *Phys. Rev. Lett.* 90 (2003) 047403.
- [7] S. Tanaka, V. Chernyak, S. Mukamel, *Phys. Rev. A* 63 (2001) 63405.
- [8] S. Mukamel, *Principles of Nonlinear Optical Spectroscopy*, Oxford Press, New York, 1995.
- [9] S. Tanaka, S. Mukamel, *Phys. Rev. A* 67 (2003) 033818.
- [10] J.R. Heath, M.A. Ratner, *Phys. Today* 56 (2003) 43.
- [11] J. Jortner, M. Ratner (Eds.), *Molecular Electronics*, Blackwell Scientific Publications, 1997.
- [12] T. Minami, S. Tretiak, V. Chernyak, S. Mukamel, *J. Lumin.* 87–89 (2000) 115.
- [13] S. Mukamel, *Nature* 388 (1997) 425.
- [14] S. Mukamel, S. Tretiak, T. Wagersreiter, V. Chernyak, *Science* 277 (1997) 781.
- [15] D.S. Chemla, J. Shah, *Nature* 411 (2001) 549.
- [16] A. Okada, V. Chernyak, S. Mukamel, *J. Phys. Chem. A* 102 (1998) 1241.
- [17] F.C. Grozema, Y.A. Berlin, L.D.A. Siebbles, *Int. J. Quantum Chem.* 75 (1999) 1009.
- [18] J. Jortner, M. Bixon, A.A. Voityuk, N. Rösch, *J. Phys. Chem. A* 106 (2002) 7599.